Multichannel Metasurface for Simultaneous Control of Holograms and Twisted Light Beams

Multi-channel metasurface for simultaneous control of holograms and twisted light beams

Chunmei Zhang[1⊥], Fuyong Yue[1⊥], Dandan Wen[1⊥], Ming Chen[2], Zhengren Zhang[1, 3], Wei Wang[1†], Xianzhong Chen[1*]

1. *SUPA, Institute of Photonics and Quantum Sciences, School of Engineering and Physical Sciences, Heriot-Watt University, Edinburgh, EH14 4AS, UK*
2. *Guangxi Experiment Center of Information Science, Guilin 541004, China*
3. *School of Science, Chongqing Jiaotong University, Chongqing 400074, China*

Abstract

In terms of system integration and device miniaturization, a single optical device that can possess more tunable functionalities in multiple channels is desirable. As a proof of concept, we experimentally demonstrate such an ultrathin optical device that can simultaneously realize polarization-controllable hologram and superposition of orbital angular momentum (OAM) in multiple channels. By continuously controlling the polarization state of the incident light, the polarization-dependent holographic images in two channels along the horizontal direction and the continuous control of OAM superposition in two channels along the vertical direction are realized. The uniqueness of the device lies in that both the superpositions of OAM states and the holographic images are controlled at the same time. This novel device provides a fast and efficient tool for simultaneous control of hologram and manipulation of OAM supposition in various channels, which significantly simplifies the experimental system and is of importance for the current efforts in the field of information optics, security, quantum science and fundamental physics.

Key words: Metasurface, multiple channels, tunable functionality, optical hologram, orbital angular momentum, simultaneous manipulation

⊥ These authors contribute equally to this work.

* Email: x.chen@hw.ac.uk
† Email: w.wang@hw.ac.uk

An optical device with multiple functionalities can perform more than one function, which is desirable for device miniaturization and system integration. While there have been great progress in the miniaturization of optical elements, current photonic integration largely consists of discrete components[1]. On the other hand, for optical systems to continue to be established as economically viable in a range of emerging application areas, it is necessary to continue the trend of miniaturization and integration. To meet the growing requirement of system integration, it is of great importance and interest to develop ultrathin optical devices that integrate multiple functionalities into one device while preserving their independent functionalities.

In recent years, metasurfaces, or planar metamaterials with subwavelength thickness, have aroused considerable interest due to their capability of arbitrary control of light propagation[2-7]. A metasurface consisting of a single layer or few-layer stacks of artificial planar structures, enables us to engineer the spatial distribution of the amplitude, phase and polarization with subwavelength resolution, making it possible to circumvent the design limitation of conventional devices, which is based on the accumulated optical path. Benefiting from the unprecedented capability in manipulating light propagation, metasurfaces have been used to develop optical devices with multiple functionalities, including polarization-sensitive hologram[8], integration of lens and hologram[9], and nonlinear metasurface holograms[10]. Light can be twisted like a corkscrew around its axis of travel. It is well known that the spin angular momentum (SAM) of light is associated with light's circular polarization. Unlike SAM, a twisted light beam with an orbital angular momentum (OAM) has a helical phase structure, which has attracted much attention due to its promising applications in particle trapping[11], optical communication[12, 13], quantum science and metrology[14, 15]. For example, the OAM can provide a new degree of freedom for multiplexing and possesses unlimited eigenstates, dramatically increasing the capacity of optical communication systems. OAM entangled light beams are good candidates for high capacity, high security communication systems. Various methods for vortex beam generation have been demonstrated[16-18]. However, there are technical challenges to manipulate superposition of light beams with OAMs[16~~16~~19]. For example, the currently available experimental system is very complex and bulky, and the aberrations in the system and the misalignment of the optical elements lead to poor performance of the system. More recently, an efficient approach to generate multiple OAM light beams and arbitrarily control their superpositions was experimentally

demonstrated[17-20]. The advance in polarization-sensitive metasurface holograms and polarization-controllable OAM superposition provides a new approach to realize a multi-channel device with tunable functionalities. Although metasurface devices with multiple functionalites or multiple channels are in their infancy, they offer in the long run major opportunities if we can integrate multiple channels and multiple tuneable functions to a single ultrathin flat nanostructured device.

Here, we experimentally demonstrate an ultrathin optical device that can simultaneously realize polarization-controllable hologram and superposition of OAM in multiple channels. By continuously controlling the polarization state of the incident light, the polarization-dependent holographic images in two channels along one direction and the manipulation of OAM superposition in two channels along the orthogonal direction are realized. Not only the superpositions of OAM states but also the dynamic change of the holographic images can be manipulated at the same time. The easy and direct control of functionalities in multiple channels might become very important for future development of advanced multifunctional devices, which can further push the limit of functionality density.

Design and Results

Figure 1a shows the schematic of experimental setup and expected results based on the designed metasurface device that can simultaneously control the holographic images and the OAM superposition. The arbitrary control of the superpositions of various light beams with OAM and polarization-controllable holograms can be realized in two vertical channels and two horizontal channels, respectively. A polarizer and a quarter waveplate (QWP) can convert a laser beam into any polarization state of the incident light. It is worth mentioning that both polarizer and QWP can be rotated in the plane perpendicular to the direction of light propagation to generate an arbitrarily polarized beam of the incident laser light. Two separate holographic images and two OAM light beams with a topological charge $\ell = 1$ (or -1) (see Fig. 1(a)) are predicted when a metasurface device is illuminated with an input light beam with pure circular polarization, i.e., right circular polarization (RCP) or left circular polarization (LCP). An OAM beam with a topological charge of ℓ has a 'doughnut' intensity profile with a dark area in the beam center. However, the two holographic images will overlap and OAM superposition will occur upon the illumination of a light beam with

elliptical polarization since it can be decomposed into a LCP light beam and a RCP light beam. Figure 1b shows the simulation results for the incident light with linear polarization (LP). Under the illumination of LCP light, Gerchberg-Saxon method is adopted to generate the phase profile for the hologram, which is used to reconstruct the holographic image along the horizontal direction. When the helicity of the incident light is changed from LCP to RCP, the flipped phase profile is used to reconstruct the holographic image. For the incident LP light, the holographic image is the superposition of above two holographic images. The intensities of two overlapping images are the same (see Fig. 1(b)) since the linearly polarized light contains a LCP light beam and a RCP light beam with equal intensities. Similarly, the generated OAM pattern along the vertical direction is the superposition of two OAM modes with opposite topological charges for the incident LP light. It is worth mentioning that the simulation result for OAM is enlarged for display purpose only. The two vertical channels are used to produce two superpositions of OAM states with $\ell = 1$ and $\ell = -1$. It should be noted that the combination of $\left| R, \quad \ell = 1 \right\rangle$ and $\left| L, \quad \ell = -1 \right\rangle$ with equal power can generate a radially polarized vector beam, which is characterized by passing through a rotating polarizer. The transmitted intensity profile with two petals is the signature of the generated radially polarized vector beam.

To realize the tunable multi-channel optical device with different functionalities, two metasurfaces (one for two holographic images along the horizontal direction and one for two OAM beams along vertical direction) are designed to operate with opposite incident helicities and merged together with a displacement vector of (d/2, d/2), as detailed in Fig. 2a. Where d is the distance between neighboring nanorods with a value of 424 nm along both x and y directions. There are two separate metasurfaces which can generate two different types of required phase profiles, but the size of the sample before and after metasurface merging is the same and the equivalent pixel size in the merged metasurface is 300 nm×300 nm.

In order to mathematically describe the designed phase distribution generated by the metasurface, the coordinate system in Fig. 2a can be rotated counterclockwise through an angle 45^{o}. The new coordinates of the point (x, y) are described by:

$$\begin{bmatrix} x' \\ y' \end{bmatrix} = \frac{\sqrt{2}}{2} \begin{bmatrix} 1 & -1 \\ 1 & 1 \end{bmatrix} \begin{bmatrix} x \\ y \end{bmatrix} \quad (1)$$

where (x', y') are the coordinates of the point after rotation.

The general phase distribution for the transmission function of the device can be written as follows:

$$\Phi(x', y') = 0.5[1 + (-1)^{m+n}]\Phi_{OAM}(x', y') + 0.5[1 - (-1)^{m+n}]\Phi_{Holo}(x', y') \quad (2)$$

where (x', y') here is the location of the nanorods in the new coordinate system, $m = \sqrt{2}x'/d$, $n = \sqrt{2}y'/d$, d = 424 nm. $\Phi_{OAM}(x', y')$ and $\Phi_{Holo}(x', y')$ are the generated phase profiles for the off-axis OAM states and the hologram, respectively.

In this project, we leverage on the recent advances in broadband reflective-type configuration and geometric metasurface to develop the designed device. The adopted metasurface consists of three layers: gold nanorod array on the top (30 nm), a gold background layer (150 nm) on the silicon substrate and a SiO_2 spacer (85 nm) sandwiched between them (shown in Fig. 2(b)). Pancharatnam-Berry (PB) phase is a geometrical phase associated with the polarization of light[21,22], which is realized here by the metasurface [8,23]. When the polarization of a beam traverse a closed loop on the Poincare sphere, the final state differs from the initial state by a phase factor equal to half the area encompassed by the loop on the sphere. Upon the illumination of a RCP light beam, the emitted light from the metasurface with same circular polarization picks up an abrupt phase change $2\varphi(x, y)$ (PB phase), where $\varphi(x, y)$ is the spatial distribution of orientation angle of the nanorods. When the polarization state of incident light is changed from RCP to LCP, the abrupt phase change is flipped to $-2\varphi(x, y)$. Geometric metasurfaces consisting of nanorod array provide an efficient way to modify not only the phase profile of light in a space-variant manner at subwavelength resolution, but also the polarization profile.

In order to reconstruct two symmetrically distributed off-axis holographic images along the horizontal direction, Gerchberg−Saxton algorithm is adopted to generate the required phase profile. Both images ('H' and 'W') have a projection angle of ($8.71^\circ \times 12.02^\circ$) and an off-axis angle of 11.10° in the imaging area (see Fig. 2c). To realize OAM superposition along the vertical direction, the

phase distribution of off-axis OAM states is described as

$$\Phi_{OAM}(x,y) = \arg(\sum_{j=1}^{2} E_j \exp(i(\ell_j \theta + \Delta\varphi_{j,y}))) \quad (3)$$

Where $j = 1,2$ means totally there are two OAM states, E_j is the amplitude component of OAM state ℓ_j, θ is the azimuthal angle and $\Delta\varphi_{j,y}$ is phase difference between neighboring pixels to generate a phase gradient along the *y* direction, which results in the off-axis deflection for the OAM mode of interest. It is worth mentioning that the off-axis deflection here is only introduced along the *y* direction (vertical direction) since there are holographic images along the *x* direction (horizontal direction). The phase difference between neighbouring pixels to generate off-axis phase gradient for OAM states is $\pi/5$ here, and the relevant off-axis angle of OAM patterns is 12.3° (See Fig. 2c). The topological charges for the two OAM beams have same value $\ell = 1$ upon the illumination of RCP light.

To experimentally verify the proposed device, we fabricate the design reflective-type metasurface consisting of nanorods with spatially varying orientation (Fig. 2d). The designed metasurfaces are fabricated using standard electron-beam lithography, metal deposition and lift-off process. A silicon substrate is firstly deposited by a gold background layer (150 nm), then followed by a SiO_2 spacer (85 nm) using an electron beam evaporator. The nanostructures are defined on the poly methyl methacrylate (PMMA) film by EBL (Raith PIONEER). Prior to gold film (30 nm) deposition, a titanium layer of ~ 3 nm is deposited on the silicon dioxide (SiO_2) layer for adhesion purpose. Finally, the metasurfaces structure is achieved by a subsequent lift-off procedure.

The experimental setup to characterize the fabricated metasurface device is shown in Fig.1a. The sample is mounted on a 3D translation stage, allowing for fine adjustment. The incident light at the wavelength of 640 nm is from a tunable supercontinuum laser source (NKT-SuperK EXTREME). An experimental setup consisting of a polarizer, a quarter-wave plate, a white paper board with an opening (diameter 6 mm) is used to generate the required polarization state. Upon the illumination of pure LCP light, two separate holographic images of ‘H’ pattern on the left and the ‘W’ pattern on the

right of the screen along the horizontal direction are clearly observed when viewed from the sample, while the two ‘donut’-shaped OAM patterns are symmetrically located along the *y* direction, as shown in Fig. 3a. Since the sign of the phase profile can be flipped by controlling the helicity of the incident light, the ‘H’ and ‘W’ pattern will be swapped in horizontal direction and flipped in vertical direction when the helicity of the incident light is changed from LCP to RCP (shown in Fig. 3b). Meanwhile, the propagating directions of two generated OAM beams are swapped with respect to the surface normal of the metasurface, and the signs of two topological charges are flipped. However, no swapped OAM beams are observed since these two OAM states in this work are exactly the same. In comparison with the simulated results, the lack of circular symmetry in the measured shape of the vortex beams is mainly due to the imperfection of the optical measurement system (e.g., misalignment). In order to further characterize the purity of the OAM beams, the simulated and experimentally measured results of the transmitted intensity profile (middle and right columns in Fig. 3) after the generated OAM beams pass through a polarizer are given as well. No clear difference before and after passing through the polarizer indicates the OAM beams with high purity.

An arbitrary polarized light beam can be considered as the superposition of two circularly polarized beams with opposite helicity, which can be described as

$$\Psi = A \cdot e^{i\vartheta} \left| R \right\rangle + B \cdot e^{-i\vartheta} \left| L \right\rangle \tag{4}$$

Where A and B denote the amplitude coefficients of RCP and LCP light, 2ϑ represents the relative phase difference between the two circular polarization states. The simulated and measured results for five polarization states of the incident light, including RCP, right-handed elliptical polarization (REP), linear polarization (LP), left-handed elliptical polarization(LEP) and LCP are given in Fig.4. Under the illumination of pure RCP light at the wavelength of 640nm, two reconstructed clear images of flipped ‘W’ and ‘H’ lie on the left and right sides of the image plane, respectively. It is worth mentioning that ‘H’ and flipped ‘H’ are the same. The distance between the screen and the metasurface sample is about 15 mm. Both holographic images (flipped ‘W’ and ‘H’) are changed to their centro-symmetric counterparts (‘H’ and ‘W’) when the light polarization is switched from RCP to LCP. However, when the elliptically or linearly polarized light impinges on the metasurface sample, the two images (mentioned above) overlap. When REP light is used, the left pattern with

higher intensity of flipped ‘W’ and lower intensity of ‘H’, while the right pattern has higher intensity pattern of ‘H’ and lower intensity pattern of ‘W’ , and vice versa for the LCP light. The intensities of the two overlapping images rise and fall according to the ellipticity of various incident polarized light, which is realized by changing the angle between the polarization axis of the polarizer and the fast axis of the quarter wave plate. When the polarization state changes to the linear polarization, the images are overlapped with the same intensity of flipped ‘W’ and ‘H’ (or ‘H’ and ‘W’).

To characterize the functionality of polarization-controlled OAM superposition, the simulated and measured intensity profiles of the OAM superposition are given in the fourth and fifth columns of Fig. 4 for the corresponding polarization states of the incident light. By continuously changing the polarization state of the light, the evolution process of the intensity distribution can be observed after the resultant OAM beam passes through the rotating polarizer (before the sample). When the linearly polarized (LP) light is incident onto the metasurface, the resultant output beams are the superposition of $|R, l=1\rangle$ and $|L, l=-1\rangle$ with equal power, which is a radially polarized vector beam that has been found in many applications due to its unique properties[20,24]. It is worth mentioning that there is a clear gap between the two petals for linear polarization of the incident light.

Discussion

The uniqueness of our design lies in the design combination of multiple functionalities and multiple channels to experimentally realize the polarization-controlled OAM superposition and hologram on a single metasurface device. The alliance between functionality and channel can dramatically increase the density of functionality and shrink the size of the device, which can push the limit of device miniaturization and system integration. In addition, the advantages such as subwavelength resolution, broadband and compactness may have a broad impact in the areas of photonics, quantum sciences, and fundamental physics. Superposition of optical beams with opposite circular polarizations and orbital angular momenta can be used to create a light beam with non-trivial polarization and phase properties. The linear combination of equal-weighted RCP optical vortex beam with topological charge $\ell = 1$ and LCP optical vortex beam with topological charge $\ell = -1$ can generate a radial vector beam (see Fig. 5), which has been applied in metrology[18,25], lithography[14], and quantum memory[19,26]. The intensity profile with two petals will be rotated if the transmission axis of the polarizer is

changed, as detailed in Fig. 5b. This nanodevice provides the ability to simultaneously control the superpositions of various OAM states and the hologram pattern, by simply controlling the polarization states of incident light without any additional optical devices.

The efficiency of the device is defined by the total power of the output light from the four channels divided by the power of incident light. The measured efficiency at 640 nm is around 9%, which agrees well with the value in the reference[20]. The efficiency at 640 nm can be improved by replacing gold with silver in this design[8] or using dielectric metasurfaces[27]. Although the metasurface is mainly characterized at the wavelength of 640 nm, it can also work in other wavelengths due to the broadband property of the reflective configuration. Experimental results at the wavelength of 530 nm are given in the supplementary.

The developed device here provides a unique method to integrate different tunable functionalities into a single nanodevice. This approach possesses several practical and technical advantages over conventional methods. Without the metasurface device designed here, to realize the simultaneous control of hologram and superposition of OAM states of different topological charge, one must rely on a complicated experimental setup consisting of beam-splitters, prisms, mirrors etc. Here, only a single device can easily complete the complicated task, which avoids the technical hassles (e.g., misalignment, aberration) caused by the conventional optical systems.

Conclusion

In a word, we experimentally demonstrate a metasurface device that can realize polarization-dependent hologram and continuously control the superposition of orbital angular momentum in multiple channels. By controlling the polarization state of incident light, different superpositions of OAM states and holographic images are realized. Good agreement between the simulated and experimental measured results is found. The developed device provides a new tool to modify the polarization and phase simultaneously. The alliance between multiple functionalities and multiple channels dramatically increases the density of functionalities, which can further push the limit of device miniaturization and system integration.

Acknowledgements

This work is supported by the Engineering and Physical Sciences Research Council of the United Kingdom (Grant Ref: EP/P029892/1 and EP/M003175/1). M. C. would like to thank the support from National Natural Science Foundation of China (No. 61640409). Z.Z. acknowledges the financial support from the China Scholarship Council (Grant No. 201608500036).

REFERENCES

(1) Zentgraf, T.; Valentine, J.; Tapia, N., Li, J.; Zhang, X. An optical "Janus" device for integrated photonics. *Adv. Mater.*, **2010**, 22, 2561-2564.

(2) Yu, N.; Genevet, P.; Kats, M. A.; Aieta, F.; Tetienne, J. P.; Capasso, F.; Gaburro, Z. Light propagation with phase discontinuities: generalized laws of reflection and refraction. *Science*, **2011**, 334, 333-337.

(3) Kildishev, A. V.; Boltasseva, A.; Shalaev, V. M. Planar photonics with metasurfaces. *Science*, **2013**, 339, 1232009..

(4) Chen, X.; Huang, L.; Mühlenbernd, H.; Li, G.; Bai, B.; Tan, Q.; Jin, G.; Qiu, C.; Zhang, S.; Zentgraf, T. Dual-polarity plasmonic metalens for visible light. *Nat. Commun.* **2012**, 3, 1198.

(5) Zheng, G.; Mühlenbernd, H.; Kenney, M.; Li, G.; Zentgraf, T.; and Zhang, S. Metasurface holograms reaching 80% efficiency. *Nat. nanotech.*, **2015**, 10, 308-312.

(6) Yin, X.; Ye, Z.; Rho, J.; Wang, Y.; Zhang, X. Photonic spin Hall effect at metasurfaces. *Science*, **2013**, 339, 1405-1407.

(7) Sun, S.; He, Q.; Xiao, S.; Xu, Q.; Li, X.; Zhou, L. Gradient-index meta-surfaces as a bridge linking propagating waves and surface waves. *Nat. Mater.*, **2012**, 11, 426-431.

(8) Wen, D.; Yue, F.; Li, G.; Zheng, G.; Chan, K.; Chen, S.; Chen, M.; Li, K. F.; Wong, P. W. H.; Cheah, K.W.; Pun, E. Y. B.; Zhang, S. Chen, X. Helicity multiplexed broadband metasurface holograms. *Nat. Commun.* **2015,** 6, 8241.

(9) Wen, D.; Chen, S.; Yue, F.; Chan, K.; Chen, M.; Ardron, M.; Li, K. F.; Wong, P. W. H.; Cheah, K.W.; Pun, E. Y. B.; Li, G.; Zhang, S.; Chen, X. Metasurface device with helicity-dependent functionality. *Adv. Opt. Mater.*, **2016**, 4, 321-327.

(10) Ye, W.; Zeuner, F.; Li, X.; Reineke, B.; He, S.; Qiu, C. W.; Liu, J.; Wang, Y.; Zhang, S.; Zentgraf, T. Spin and Wavelength Multiplexed Nonlinear Metasurface Holography. *Nat.*

Commun., **2016**, 7, 11930.

(11) Padgett, M.; Bowman, R. Tweezers with a twist. *Nat. Photonics*, 2011, 5, 343-348.

(12) Willner, A. E.; Huang, H.; Yan, Y.; Ren, Y.; Ahmed, N.; Xie, G.; Bao, C.; Li, L.; Cao, Y.; Zhao, Z.; Wang, J.; Lavery, M. P. J.; Tur, M.; Ramachandran, S.; Molisch, A. F.; Ashrafi, N.; Ashrafi S. Optical communications using orbital angular momentum beams. *Adv. in Opt. and Photonics*, **2015**, 7, 66-106.

(13) Wang, J.; Yang, J. Y.; Fazal, I. M.; Ahmed, N.; Yan, Y.; Huang, H.; Ren, Y.; Yue, Y.; Dolinar, S.; Tur, M; Willner, A. E. Terabit free-space data transmission employing orbital angular momentum multiplexing. *Nat. Photonics*, 2012, 6, 488-496.

(14) Vaziri, A.; Weihs, G.; Zeilinger, A. Superpositions of the orbital angular momentum for applications in quantum experiments. *J. of Opt. B: Quantum and Semiclassical Optics*, **2002**, *4*, S47

(15) Marrucci, L.; Karimi, E.; Slussarenko, S.; Piccirillo, B.; Santamato, E.; Nagali, E.; Sciarrino, F. Spin-to-orbital conversion of the angular momentum of light and its classical and quantum applications. *J. Opt.*, **2011**, *13*, 064001.

(16) Marrucci, L.; Manzo, C.; Paparo, D. Optical Spin-to-Orbital Angular Momentum Conversion in Inhomogeneous Anisotropic Media. *Phys. Rev. Lett.*,**2006**, *96, 163905.*

(17) Tam, A.M.W. et.al., *Bifocal Vortex Lens with Sorting of the Generated Nonseparable Spin-Orbital Angular-Momentum States, Phys. Rev. Appl.*, **2017**, *7, 034010* .

(18) Allen,L.; Beijersbergen, M.W; Spreeuw, R.J.C; Woerdman, J.P. *Orbital angular momentum of light and the transformation of Laguerre-Gaussian laser modes*, *Phys. Rev. A,* **1992,** *45, 8185-8189.*.

(19) Fickler, R.; Krenn, M.; Lapkiewicz, R.; Ramelow, S.; Zeilinger, A. Real-time imaging of quantum entanglement. Scientific reports. *Sci. Rep*. **2013**, *3,* 1914.

(20) Yue, F.; Wen, D.; Zhang, C.; Gerardot, B. D.; Wang, W.; Zhang, S.; Chen, X. Multichannel Polarization‐Controllable Superpositions of Orbital Angular Momentum States. *Adv. Mater.*, **2017**, 29, 1603838.

(21) Pancharatnam, S. Generalized theory of interference and its applications Part I. Coherent pencils, *Proc. Indian Acad. Sci. A*, **1956**, 44, 247-262.

(22) Berry, M. Quantal phase factors accompanying adiabatic changes, *Proc. R. Soc. A*, **1984**, 392, 45-47.

(23) Huang, L.; Chen, X.; Muhlenbernd, H.; Li,G.;Bai, B.;Tan, Q.; Jin,G.;Zentgraf, T.;Zhang, S. Dispersionless phase Discontinuities for Controlling Light Propagation. *Nano Lett.*, **2012**, 12, 5750-5755.

(24) Zhan, Q. Trapping metallic Rayleigh particles with radial polarization. *Opt. express*, **2004**, 12, 3377-3382.

(25) Lavery, M. P.; Speirits, F. C.; Barnett, S. M.; Padgett, M. J. Detection of a spinning object using light's orbital angular momentum. *Science,* **2013**, *341*, 537-540.

(26) Nicolas, A.; Veissier, L.; Giner, L.; Giacobino, E.; Maxein, D.; Laurat, J.; A quantum memory for orbital angular momentum photonic qubits. *Nat. Photonics,* **2014**, 8, 234-238.

(27) Khorasaninejad, M.; Chen, W.T., Devlin; R. C.; Oh, J.; Zhu, A.Y.; and Capasso, F., Metalenses at visible wavelengths: Diffraction-limited focusing and subwavelength resolution imaging, *Science*, **2016**, 352,1190-1194.

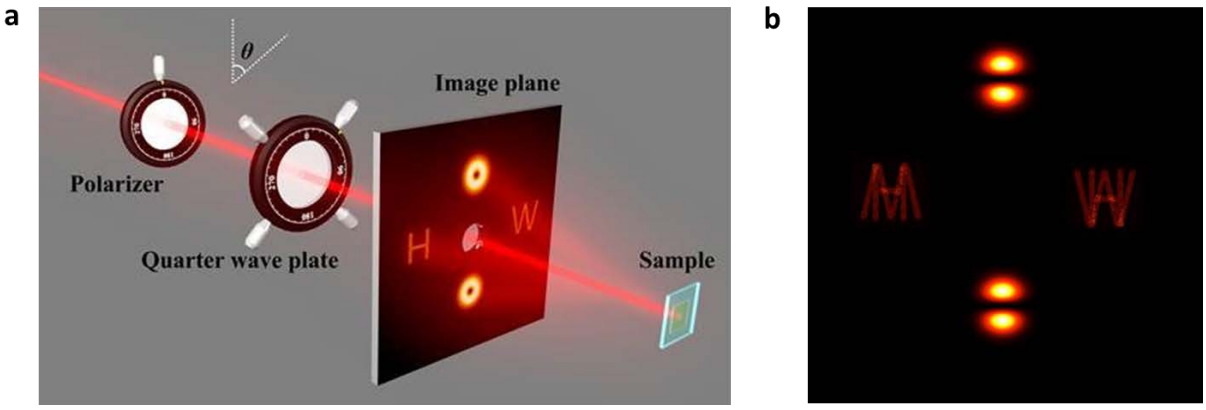

Figure 1 Schematic illustration of simultaneous control of hologram and superposition of orbital angular momentum (OAM). (a) Under the illumination of LCP light, the holographic images ‘H’ and ‘W’ are reconstructed on the left and right side along the horizontal direction, respectively. Two pure OAM beams with the same topological charges are generated along the vertical direction. (b) The simulation results for the incident light with linear polarization. The intensities of two overlapping holographic images are the same and the two superpositions of OAM states with $\ell = 1$ and $\ell = -1$ are in the vertical channel. The superposition of $|R, \quad \ell = 1\rangle$ and $|L, \quad \ell = -1\rangle$ with equal components can generate a radially polarized vector beam, which is verified by the resultant two petals after the light beam passes through a polarizer with a transmission axis along the vertical direction.

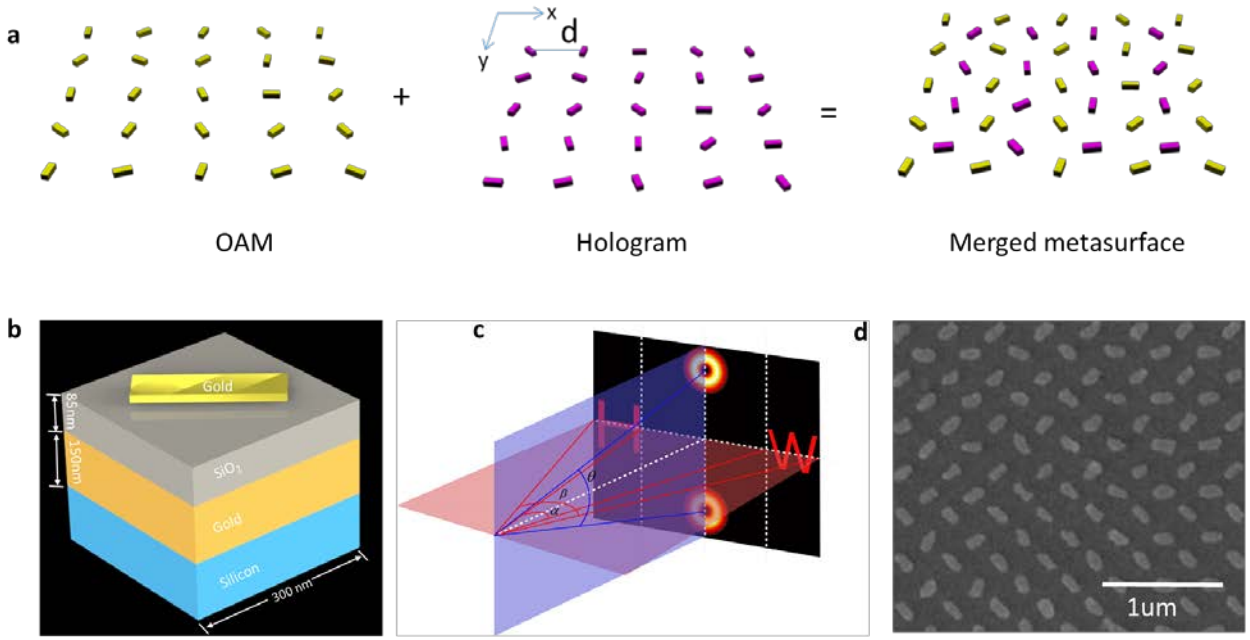

Figure 2 Design schematic of the multi-channel metasurface device with tunable functionalities. **(a)** One metasurface for two holographic images along the horizontal direction and the other for two OAM beams along vertical direction are merged together with a displacement vector of (d/2, d/2). d is the distance between neighboring antennas with a value of 424 nm. The size of the sample is still the same and the equivalent pixel size is 300 nm× 300 nm. (b) The reflective-type metasurface consists of gold nanorods with spatially varying orientations on the top, a SiO_2 spacer (80 nm) and a gold background layer (150 nm) resting on a silicon substrate. (c) Geometric parameters of the projected holographic images and OAM beams that correspond to the merged hologram. The full off-axis angle α, β and γ are designed to be 22.2°, 32.5° and 24.6°, respectively. (d) SEM image of the fabricated metasurface. The scale bar is 1 μm. The equivalent pixel size is 300×300 nm^2.

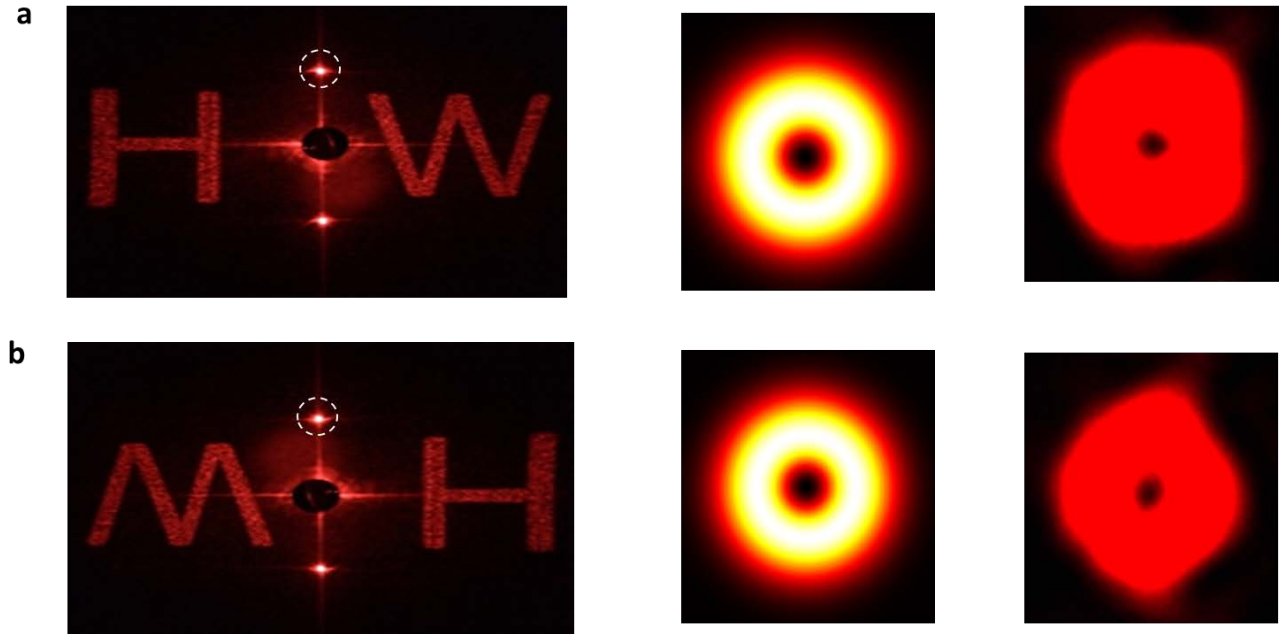

Figure 3 **Dependence of experimental results on the helicity of the incident light.** The experimentally obtained images for the incident light with (a) LCP and (b) RCP. The incident light impinges normally onto the metasurface and the reconstructed images are projected onto the image plane. The screen is a white paper board with an opening (diameter 6 mm) in the middle, which allows the incident light and zero order reflected light passing through. The wavelength of the incident light is 640 nm. The dashed circles mark the generated OAM beam. Simulated and measured intensity profiles of the OAM beam for (c) LCP and (d) RCP after the light beam passes through the polarizer with the transmission axis along the vertical direction.

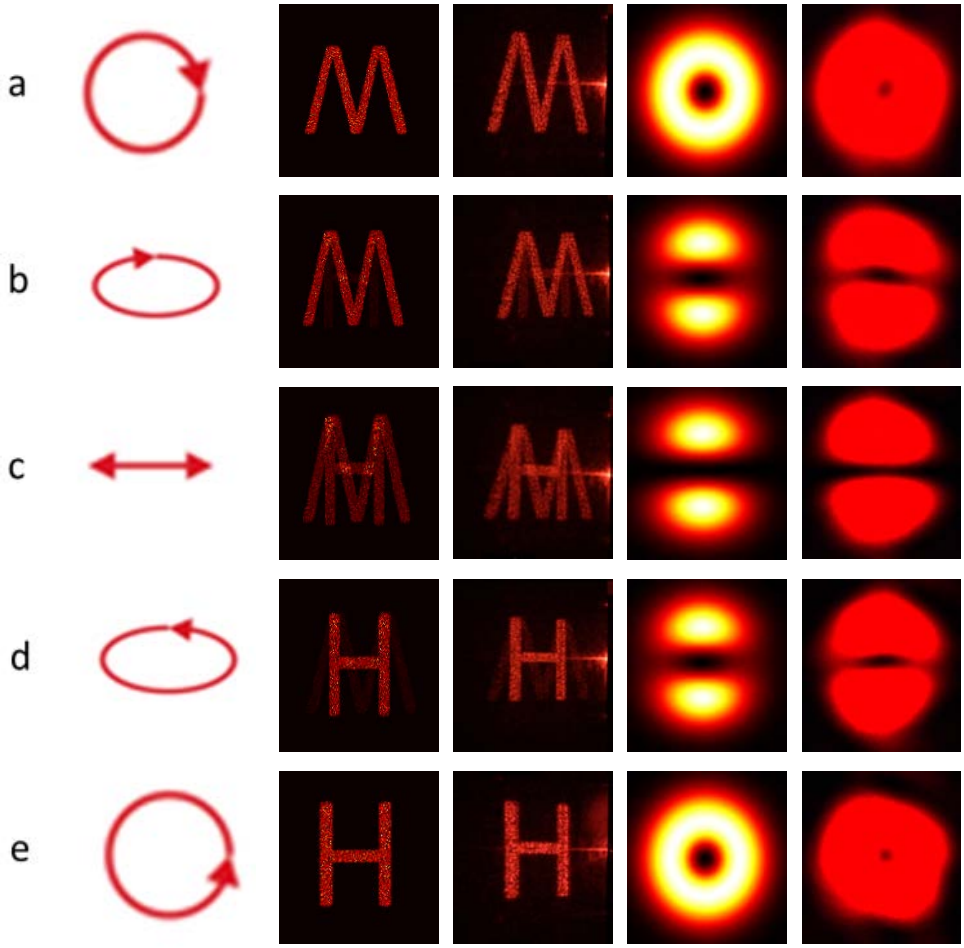

Figure 4 Experimentally measured results and simulation results versus polarization states of the incident light at 640 nm. The polarization states of the incident light are chosen to be (a) RCP, (b) right-handed elliptically polarized, (c) linearly polarized, (d) left-handed elliptically polarized and (e) LCP. The second and third columns represent the simulated and experimental results of holographic images in one channel. The fourth and fifth columns show the simulated and measured results for the generated intensity profiles for corresponding polarization states after the resultant OAM beam passes through the linear polarizer whose transmission axis is along the vertical direction.

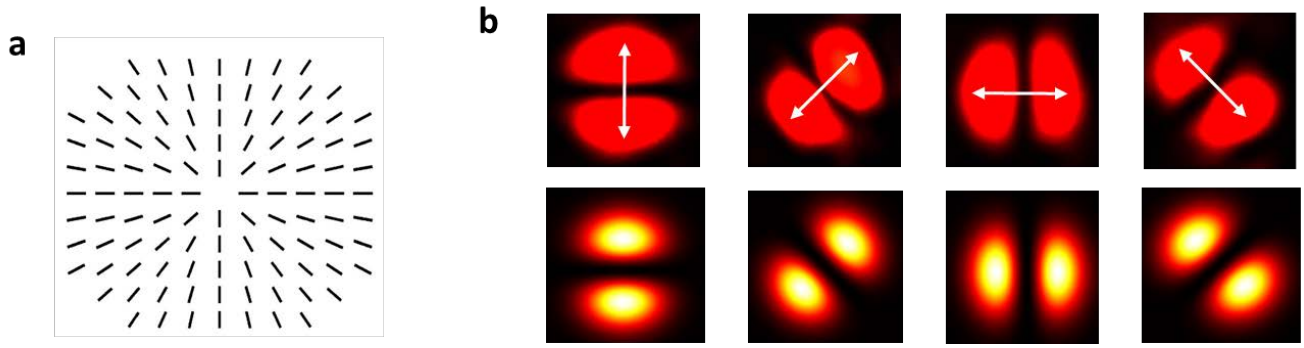

Figure 5 Polarization profile of a radially polarized vector beam and intensity profile of the resultant beam for the incident light with linear polarization. (a) Polarization distribution of the radially polarized vector beam. (b) Under the illumination of linearly polarized light beam, the resultant beam from the superposition of two OAM beams with topological charges $\ell = 1$ and $\ell = -1$ in the vertical channel is a radially polarized vector beam. To characterize these beams, two petals in the intensity profile are predicted and observed after the light beam passes through the polarizer. The two petals are rotated when the transmission axis of the polarizer is changed. The white double-headed arrows show the direction of the analyzing polarizer's axis.

For Table of Contents Use Only

Multi-channel metasurface for simultaneous control of holograms and twisted light beams

Chunmei Zhang[1⊥], Fuyong Yue[1⊥], Dandan Wen[1⊥], Ming Chen[2], Zhengren Zhang[1, 3], Wei Wang[1†], Xianzhong Chen[1*]

1. *SUPA, Institute of Photonics and Quantum Sciences, School of Engineering and Physical Sciences, Heriot-Watt University, Edinburgh, EH14 4AS, UK*
2. *Guangxi Experiment Center of Information Science, Guilin 541004, China*
3. *School of Science, Chongqing Jiaotong University, Chongqing 400074, China*

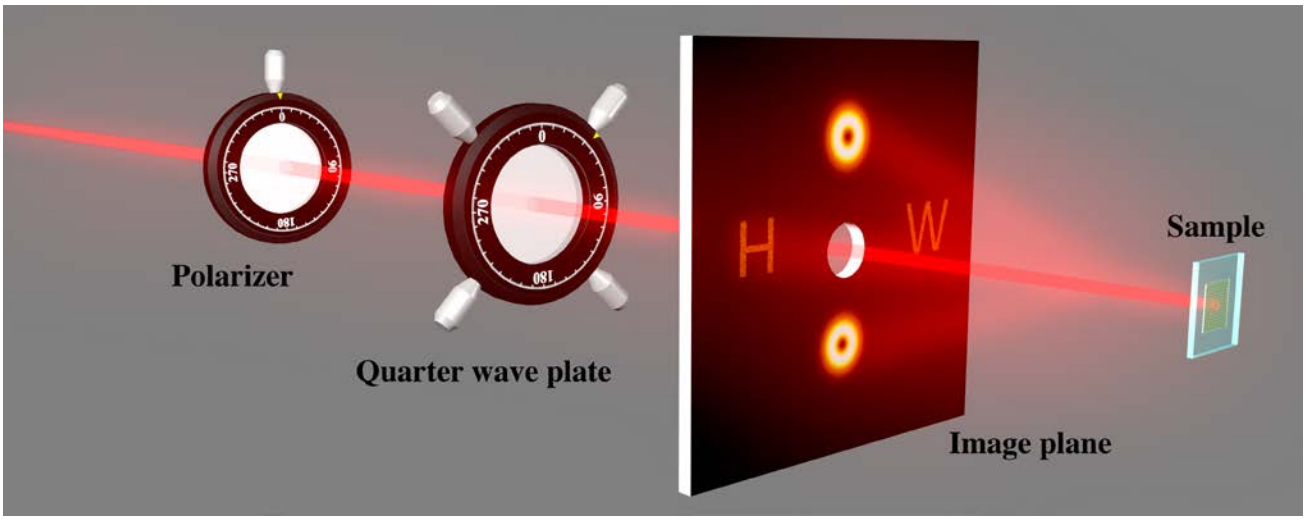

Description:

This schematic shows the experimental setup and expected results based on the designed metasurface device that can simultaneously control the holographic images and the OAM superposition. Under the illumination of light with circular polarizations, the holographic images are reconstructed along the horizontal direction and two pure OAM beams with the same topological charges are generated along the vertical direction. By controlling the polarization state of the incident light with a polarizer and a quarter waveplate, the arbitrary control of the superpositions of various light beams with OAM and polarization-controllable holograms are realized in two vertical channels and two horizontal channels, respectively.